18th International Conference on Information Fusion
Washington, DC - July 6-9, 2015

Configuration Selection for Fusion of Range and Doppler Measurements from Multistatic Radars for Air Collision Warning

Wenbo Dou, Peter Willett and Yaakov Bar-Shalom
Department of Electrical and Computer Engineering
University of Connecticut
Storrs, CT 06269
Email: {wed12005,willett,ybs}@engr.uconn.edu

***Abstract*—A requisite for unmanned aircraft systems (UAS) to operate within a controlled airspace is a capability to sense and avoid collisions with non-cooperative aircraft. Ground-based transmitters and UAS-mounted receivers are preferred due to the limitations on the size, weight and power of UAS. This paper assumes a constant velocity motion of an intruder (target) aircraft and presents a method to estimate the state (motion parameters — position and velocity) of the target so as to predict the closest point of approach. Bistatic range and Doppler are assumed the only measurements available, with the employment of low-cost omni-directional antennas. Several configurations are investigated from a parameter observability point of view. It turns out that one needs three transmitters in a general three-dimensional (3-D) scenario to achieve very good observability of the target motion parameter. With the assumption that the target is at the same altitude as the ownship, one has a two-dimensional (2-D) scenario in which two transmitters are required to have good observability. Simulation results show that the maximum likelihood (ML) estimate of the target parameter using iterated least squares (ILS) search is statistically efficient in both multistatic configurations with good observability. The collision warning is formulated as a hypothesis testing problem using a generalized likelihood function. The warning algorithm has no missed detection of a collision event in either configuration. It has a lower false alarm rate in a 3-D scenario than in a 2-D scenario at the expense of one more ground-based transmitter.**

I. Introduction

Sense-and-Avoid (SAA) capabilities are required for unmanned aircraft systems (UAS) to operate within the national airspace. The proliferation of UAS has increased the risk of aircraft collision. The air traffic control radar beacon system works well to coordinate cooperative aircraft. Active sensing methods have to be employed for UAS to be functional against non-cooperative targets. The limitations on the size, weight and power of UAS suggest an implementation with ground based transmitters and UAS mounted receivers.

There have been numerous works on the UAS collision avoidance problem [1]. Most have emphasized avoidance algorithms [5][8][9], while sensing and estimation methods have not been extensively explored. In [7], a monostatic radar configuration in a 2-D plane with range and bearing measurements is considered for collision avoidance. In [10], a confidence corridor is mathematically constructed without any specification of the measurements.

In our previous work [6], a strategy for collision warning in a 3-D space is presented where we assume a constant velocity motion of an aircraft of interest (target/intruder) and attempt to estimate the state (position and velocity) of the target so as to predict the closest point of approach (CPA). Since an inexpensive system is the goal, only bistatic range and Doppler measurements are available. Several configurations are investigated from a parameter observability point of view. The target parameter is shown to be unobservable in a bistatic configuration (that is: one transmitter and one receiver, not co-located) and a change of course of the receiver (the "observability platform maneuver" that is the saving grace for angle-only target motion analysis (TMA)) merely improves the observability marginally. In a multistatic configuration, one has marginal observability using two transmitters but good observability with three transmitters. Simulation results show that the ML estimate of the target parameter is statistically efficient in a multistatic configuration with three transmitters.

This paper extends the previous work [6] with an inclusion of a special 2-D problem based on the assumption that the target is at the same altitude as the ownship and attempts to provide a comprehensive guideline on configuration selection for air collision warning. A few more scenarios are analyzed from the parameter observability point of view. In a bistatic configuration, the target parameter is still badly observable with an assumed target altitude. The observability is improved by a small maneuver of the ownship but is not good enough. One can have very good observability of the target motion parameter with two transmitters in a multistatic configuration under the same target and ownship altitude assumption, which turns out to be another practically useful configuration in addition to a multistatic configuration with three transmitters. Simulation results confirms the statistical efficiency of the ML estimator of the target parameter in this new useful configuration. Furthermore, the collision warning is formulated as a hypothesis testing problem using a generalized likelihood function. Monte Carlo simulation shows the collision warning algorithm using three transmitters has no missed detection of a collision and has no false alarm when the intruder and ownship altitude separation is beyond 100 m. The collision warning algorithm using two transmitters with the same altitude assumption has no missed detection of a collision, either. It has higher false alarm rates in some scenarios, however, the avoidance maneuver action caused by such false alarms can be simply accomplished if one prefers more savings.

The remaining sections of this paper are organized as follows. Section II describes and formulates a general 3-D problem and extends to a special 2-D problem. Section III analyzes several possible configurations for collision warning including some new 2-D scenarios and shows two of them are practically useful. Section IV presents the ML estimator and the collision warning algorithm. Section V confirms the efficiency of the ML estimator of the target parameter and shows the new findings on the performance of the collision warning algorithm and Section VI draws conclusions.

II. Problem Formulation

Assume a target of interest (intruder) is moving in the 3-D space with a constant velocity. The 3-D target position in Cartesian coordinates at time k is

$$\boldsymbol{\xi}(\mathbf{x},k) = \mathbf{x}_0 + kT\dot{\mathbf{x}}_0 \qquad k = 0,1,\ldots \tag{1}$$

where

$$\mathbf{x} = [\mathbf{x}_0', \dot{\mathbf{x}}_0']' = [x,y,z,\dot{x},\dot{y},\dot{z}]' \tag{2}$$

is the unknown target parameter which is a vector of dimension $n_{\mathbf{x}} = 6$ consisting of the target's position $\mathbf{x}_0$ and velocity $\dot{\mathbf{x}}_0$ in Cartesian coordinates at time $k = 0$ (or at a chosen reference time); and T is the sampling period. There are N_{TX} ($N_{\mathrm{TX}} \geq 1$) transmitters at known locations $\mathbf{u}_i = [x_{u_i}, y_{u_i}, z_{u_i}]', i = 1,\ldots,N_{\mathrm{TX}}$. At time k ($k > 0$), a moving receiver (the ownship) with known position $\mathbf{s}(k)$ and velocity $\dot{\mathbf{s}}(k)$ can obtain measurements consisting of the bistatic range [4] and the bistatic Doppler, as illustrated in Figure 1, from the ith transmitter located at $\mathbf{u}_i$ given by

$$\mathbf{z}_i(k) = \mathbf{h}_i(\mathbf{x},k) + \mathbf{w}_i(k) \qquad i = 1,\ldots,N_{\mathrm{TX}} \tag{3}$$

where

$$\begin{aligned}\mathbf{h}_i(\mathbf{x},k) &= \begin{bmatrix} r_i(k) \\ \dot{r}_i(k) \end{bmatrix} \\ &= \begin{bmatrix} \|\boldsymbol{\xi}(\mathbf{x},k)-\mathbf{s}(k)\| + \|\boldsymbol{\xi}(\mathbf{x},k)-\mathbf{u}_i\| \\ \frac{[\boldsymbol{\xi}(\mathbf{x},k)-\mathbf{s}(k)]'[\dot{\mathbf{x}}_0-\dot{\mathbf{s}}(k)]}{\|\boldsymbol{\xi}(\mathbf{x},k)-\mathbf{s}(k)\|} + \frac{[\boldsymbol{\xi}(\mathbf{x},k)-\mathbf{u}_i]'\dot{\mathbf{x}}_0}{\|\boldsymbol{\xi}(\mathbf{x},k)-\mathbf{u}_i\|} \end{bmatrix}\end{aligned} \tag{4}$$

and $\mathbf{w}_i(k)$ are the measurement noises, assumed to be independent and identically distributed zero-mean white Gaussian sequences with known covariance matrix

$$R_i = \begin{bmatrix} \sigma_r^2 & 0 \\ 0 & \sigma_{\dot{r}}^2 \end{bmatrix} \tag{5}$$

The measurement function comprising all the measurements at time k is

$$\mathbf{z}(k) = \mathbf{h}(\mathbf{x},k) + \mathbf{w}(k) \qquad k = 1,\ldots \tag{6}$$

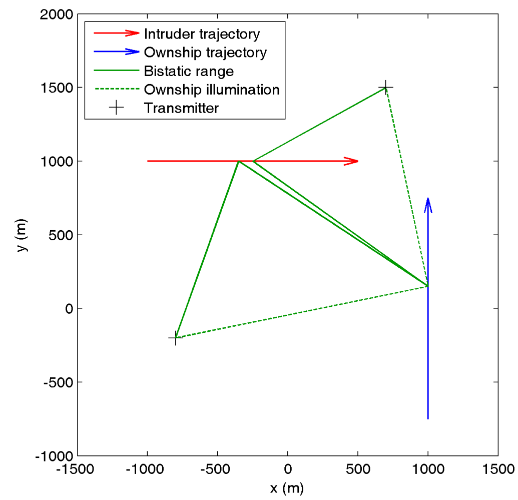

Fig. 1. A multistatic configuration in the X-Y plane

where

$$\mathbf{z}(k) = [\mathbf{z}_1(k)' \ldots \mathbf{z}_{N_{\mathrm{TX}}}(k)']' \tag{7}$$

$$\mathbf{h}(\mathbf{x},k) = [\mathbf{h}_1(\mathbf{x},k)' \ldots \mathbf{h}_{N_{\mathrm{TX}}}(\mathbf{x},k)']' \tag{8}$$

$$\mathbf{w}(k) = [\mathbf{w}_1(k)' \ldots \mathbf{w}_{N_{\mathrm{TX}}}(k)']' \tag{9}$$

and

$$\begin{aligned} R(k) &= E[\mathbf{w}(k)\mathbf{w}(k)'] \\ &= \begin{bmatrix} R_1 & \mathbf{0} & \cdots & \mathbf{0} \\ \mathbf{0} & R_2 & \cdots & \mathbf{0} \\ \vdots & \vdots & \ddots & \vdots \\ \mathbf{0} & \mathbf{0} & \cdots & R_{N_{\mathrm{TX}}} \end{bmatrix} \end{aligned} \tag{10}$$

Since both the intruder and the ownship are moving, it is important to avoid any collision between them. The goal is thus to estimate the target parameter $\mathbf{x}$ based on N frames of measurements long enough before a possible collision occurs so as to predict the CPA and presumably, to do something about it if needed.

A. Parameter Observability

We need to check observability to see whether there is sufficient information in the data. Observability requires the invertibility of the Fisher information matrix (FIM), which is given by [2]

$$J = E\left\{[\nabla_{\mathbf{x}} \ln \Lambda(\mathbf{x};\mathbf{Z})][\nabla_{\mathbf{x}} \ln \Lambda(\mathbf{x};\mathbf{Z})]'\right\}\big|_{\mathbf{x}=\mathbf{x}_t} \tag{11}$$

where $\Lambda(\mathbf{x};\mathbf{Z})$ is the likelihood function of the parameter based on the measurement set

$$\mathbf{Z} = \mathbf{z}(k)_{k=1}^{N} \tag{12}$$

and $\mathbf{x}_t$ is the true value of the parameter.

Since the measurement noises are assumed to be white, we have

$$\Lambda(\mathbf{x};\mathbf{Z})=\prod_{k=1}^{N} p\left(\mathbf{z}(k)|\mathbf{x}\right) \tag{13}$$

where

$$\begin{aligned} p\left(\mathbf{z}(k)|\mathbf{x}\right) &= |2\pi R(k)|^{-\frac{1}{2}} \\ &\cdot \exp\left(-\frac{1}{2}\left[\mathbf{z}(k)-\mathbf{h}(\mathbf{x},k)\right]' R(k)^{-1}\left[\mathbf{z}(k)-\mathbf{h}(\mathbf{x},k)\right]\right) \end{aligned} \tag{14}$$

The gradient of the log-likelihood function is

$$\nabla_{\mathbf{x}} \ln \Lambda(\mathbf{x};\mathbf{Z}) = -\sum_{k=1}^{N}\left[\nabla_{\mathbf{x}}\mathbf{h}(\mathbf{x},k)'\right] R(k)^{-1}\left[\mathbf{z}(k)-\mathbf{h}(\mathbf{x},k)\right] \tag{15}$$

Substituting (15) into (11) yields

$$\begin{aligned} J &= \sum_{k=1}^{N}\left[\nabla_{\mathbf{x}}\mathbf{h}(\mathbf{x},k)'\right] R(k)^{-1}\left[\nabla_{\mathbf{x}}\mathbf{h}(\mathbf{x},k)'\right]'\Big|_{\mathbf{x}=\mathbf{x}_{\mathrm{t}}} \\ &= \sum_{k=1}^{N}\sum_{i=1}^{N_{\mathrm{TX}}}\left[\nabla_{\mathbf{x}}\mathbf{h}_i(\mathbf{x},k)'\right] R_i^{-1}\left[\nabla_{\mathbf{x}}\mathbf{h}_i(\mathbf{x},k)'\right]'\Big|_{\mathbf{x}=\mathbf{x}_{\mathrm{t}}} \end{aligned} \tag{16}$$

If J is not invertible, then the parameter is unobservable. Otherwise, the size of confidence region for the target position [2] can be used to distinguish between marginal observability and good observability.

B. Confidence Region

Suppose an unbiased parameter estimate $\hat{\mathbf{x}}$ is obtained, then according to the Cramer Rao lower bound (CRLB), the covariance matrix is bounded from below as (if the FIM is invertible)

$$E\left[\left[\hat{\mathbf{x}}-\mathbf{x}_{\mathrm{t}}\right]\left[\hat{\mathbf{x}}-\mathbf{x}_{\mathrm{t}}\right]'\right] \geq J^{-1} \tag{17}$$

We further assume that the parameter estimation error

$$\tilde{\mathbf{x}} \triangleq \mathbf{x}_{\mathrm{t}}-\hat{\mathbf{x}} \tag{18}$$

is Gaussian distributed with covariance equal to the CRLB, that is,

$$P \triangleq E\left[\tilde{\mathbf{x}}\tilde{\mathbf{x}}'\right] = J^{-1} \tag{19}$$

The validity of (19) is confirmed in Section V.

The 3-D target position estimate at an arbitrary time t is

$$\hat{\mathbf{x}}_{\mathrm{p}}(t) = \begin{bmatrix} 1 & 0 & 0 & t & 0 & 0 \\ 0 & 1 & 0 & 0 & t & 0 \\ 0 & 0 & 1 & 0 & 0 & t \end{bmatrix} \hat{\mathbf{x}} \triangleq \Phi_{\mathrm{p}}(t)\hat{\mathbf{x}} \tag{20}$$

and the corresponding covariance is

$$P_{\mathrm{p}}(t) = \Phi_{\mathrm{p}}(t) P \Phi_{\mathrm{p}}(t)' \tag{21}$$

The normalized estimation error squared (NEES) for the target position $\mathbf{x}_{\mathrm{p}}(t)$ at t, defined as

$$\epsilon_{\mathrm{p}}(t) = \left[\mathbf{x}_{\mathrm{p}}(t)-\hat{\mathbf{x}}_{\mathrm{p}}(t)\right]' P_{\mathrm{p}}^{-1}(t)\left[\mathbf{x}_{\mathrm{p}}(t)-\hat{\mathbf{x}}_{\mathrm{p}}(t)\right] \tag{22}$$

is chi-square distributed with $n_{\mathbf{x}}/2$ degrees of freedom, that is,

$$\epsilon_{\mathrm{p}}(t) \sim \chi^2_{n_{\mathbf{x}}/2} \tag{23}$$

Let g be such that

$$P\{\epsilon_{\mathrm{p}}(t) \leq g^2\} = 1-Q \tag{24}$$

where Q is a small tail probability. Given the true target position $\mathbf{x}_{\mathrm{p}}(t)$ at t, one can say that the $100(1-Q)\%$ probability region for the predicted position at t is the ellipsoid given by

$$\left[\mathbf{x}_{\mathrm{p}}(t)-\hat{\mathbf{x}}_{\mathrm{p}}(t)\right]' P_{\mathrm{p}}^{-1}(t)\left[\mathbf{x}_{\mathrm{p}}(t)-\hat{\mathbf{x}}_{\mathrm{p}}(t)\right] = g^2 \tag{25}$$

Alternatively, given the predicted position $\hat{\mathbf{x}}_{\mathrm{p}}(t)$, (25) is the confidence region of the true position [3]. If this region is large, one has marginal observability of the target position; if the position confidence region is small, one has good observability of the target position.

C. Intruder and Ownship at the Same Altitude

If the intruder's altitude z is assumed to be known and is equal to that of the ownship, then the 2-D X-Y plane at the altitude z is of interest and everything related to the target can be considered in this 2-D space. Specifically, the target parameter to be estimated becomes

$$\mathbf{x}^{\mathrm{2D}} = [x, y, \dot{x}, \dot{y}]' \tag{26}$$

Correspondingly, the 2-D target position at an arbitrary time t is

$$\mathbf{x}_{\mathrm{p}}^{\mathrm{2D}}(t) = \begin{bmatrix} 1 & 0 & t & 0 \\ 0 & 1 & 0 & t \end{bmatrix} \mathbf{x}^{\mathrm{2D}} \tag{27}$$

The confidence region for the target position around its estimate is now an ellipse given by (25).

III. Scenarios and Observability Analysis

A radar system, which consists of three transmitters on the ground and one receiver mounted on an unmanned aircraft system (UAS) — the ownship — is used to warn of a possible collision between the UAS (ownship) and other intruder aircraft. The transmitters are located at (0 m, 1000 m, 0 m), (0 m, –1000 m, 0 m) and (1000 m, 0 m, 0 m) in Cartesian coordinates, and are denoted by TX1, TX2 and TX3, respectively. The UAS is moving at an altitude of 1500 m.

Eight collision scenarios and one non-collision scenario listed in the Table I differing in the number of transmitters, the motion of the UAS and the dimensionality of target parameter are studied here. Scenarios with the known target altitude assumption are referred to as 2-D scenarios. The rest are 3-D scenarios. Two motions of UAS are considered. In a constant velocity (CV) motion, the UAS starts moving from the point (–4500 m, 0 m, 1500 m) at time $t = 0$ s with a constant velocity $\dot{\mathbf{s}}_0 = [50\,\mathrm{m/s}, 0\,\mathrm{m/s}, 0\,\mathrm{m/s}]'$. In a two-segment CV motion, the UAS starts with a constant velocity $[43.3\,\mathrm{m/s}, -25\,\mathrm{m/s}, 0\,\mathrm{m/s}]'$ from the point (–4305.6 m, 751.7 m, 1500 m) at time $t = 0$ s for 27 s and then executes a 5° /s coordinated turn for 6 s before

TABLE I
SCENARIO SPECIFICATIONS

Scenario	Transmitters used	UAS motion	Target altitude	Collision	Semiaxis lengths of 99.9999% probability region (m)
1	TX1	CV	Unknown	Yes	3×10^9, 2020, 62
2	TX1	two-segment CV	Unknown	Yes	6468, 1660, 109
3	TX1 and TX2	CV	Unknown	Yes	1542, 50, 41
4	TX1 and TX2	two-segment CV	Unknown	Yes	1402, 51, 41
5	TX1,TX2 and TX3	CV	Unknown	Yes	50, 42, 11
6	TX1,TX2 and TX3	CV	Unknown	No	48, 43, 12
7	TX1	CV	Known	Yes	2600, 81
8	TX1	two-segment CV	Known	Yes	301, 25
9	TX1 and TX2	CV	Known	Yes	40, 8

changing to another velocity $[50\,\text{m/s}, 0\,\text{m/s}, 0\,\text{m/s}]'$ when it arrives at the location (–2850 m, 0 m, 1500 m). In all the collision scenarios, the intruder aircraft starts from the position (4500 m, 0 m, 1500 m) at time $t = 0$ s with a constant velocity $\dot{\mathbf{x}}_0 = [-50\,\text{m/s}, 0\,\text{m/s}, 0\,\text{m/s}]$ and will collide with the UAS at time $t = 90$ s. In the non-collision scenario, the altitude of the intruder aircraft is assumed to be 1600 m, which is 100 m higher than in the collision scenarios, and the CPA occurs at time $t = 90$ s. Bistatic range and Doppler measurements are made from the ownship every 1 s over a period of 60 s, which is 30 s before the CPA time. The noise standard deviations for the range and Doppler measurements are assumed to be 8.66 m and 1 m/s, respectively, at all times.

Figure 2 visualizes all the nine scenarios and plots the 99.9999% probability region, the lengths of the semiaxes of which are also shown in Table I, around the collision point or the target CPA in each scenario. Figure 3 provides the magnified view of the 99.9999% probability region in Scenarios 5, 6 and 9 where the observability is good.

In Scenario 1, the FIM is nearly singular with a condition number[1] of 18.8. The huge uncertainty ellipsoid indicates the target parameter is practically unobservable and even an efficient estimator is useless in such a situation.

In Scenario 2, the FIM is not ill-conditioned. The uncertainty ellipsoid is much smaller than in the first scenario, which indicates the change of course in the ownship trajectory improves the observability. However, the size of the uncertainty region is still quite large so that even an efficient estimator remains practically useless.

Compared with the 3-D bistatic configuration (Scenarios 1 and 2), adding a second transmitter in Scenarios 3 and 4 reduces the target localization uncertainty, although the size of the probability region is still too large to be useful. Comparison between Figures 2(c) and 2(d) indicates that the further reduction of the localization uncertainty resulting from the change of course in the ownship trajectory in the multistatic configuration is not as significant as in the bistatic counterpart.

As shown in Figure 2(e) and 2(f), the addition of a third transmitter into the multistatic configuration has significantly improved the observability of the target location, which makes the localization uncertainty as small as what is practically useful. Therefore, one needs three transmitters in a multistatic configuration to build up an efficient estimator based on which a useful collision warning algorithm can be designed.

Compared with 3-D scenarios, the knowledge of target altitude in a 2-D scenario results in a significant reduction in the uncertainty about the target localization. In Scenario 7, the size of the uncertainty region is still too large to be useful. In Scenario 8, the uncertainty region could be useful, however, it is due to the change of course of the ownship and this maneuver action itself could lead a safety situation to a dangerous collision. In Scenario 9, adding a second transmitter reduces the target localization uncertainty significantly. The size of this region is practically useful. Therefore, with the knowledge of the target altitude one needs two transmitters in a multistatic configuration to build up an efficient estimator based on which a useful collision warning algorithm can be designed.

In the sequel, collision warning is only considered in those two practically useful configurations — 3 transmitters in general 3-D scenarios and 2 transmitters with known target altitude in 2-D scenarios.

IV. The Maximum Likelihood Estimator and Collision Warning

A. Estimation of the Target Parameter

The ML estimate of the target parameter $\mathbf{x}$ in (1) is

$$\hat{\mathbf{x}}_{\mathrm{ML}} = \arg\max_{\mathbf{x}} \Lambda(\mathbf{x}; \mathbf{Z}) \tag{28}$$

where $\Lambda(\mathbf{x}; \mathbf{Z})$ is given in (13). The ILS technique [3] was used to find the ML estimate in this case. If we set (15) to zero, we will notice that there is no closed-form solution. Using a first order series expansion about an estimate $\hat{\mathbf{x}}^j$ at the end of the j-th iteration leads to an iterative scheme and the $(j+1)$-th estimate is

$$\hat{\mathbf{x}}^{j+1} = \hat{\mathbf{x}}^j + \left[(H^j)' R^{-1} H^j\right]^{-1} (H^j)' R^{-1} \left[\mathbf{z} - \mathbf{h}(\hat{\mathbf{x}}^j)\right] \tag{29}$$

[1]The condition number is $\log_{10} \frac{\lambda_{max}}{\lambda_{min}}$, where λ_{max} and λ_{min} are the largest and smallest eigenvalues of the FIM.

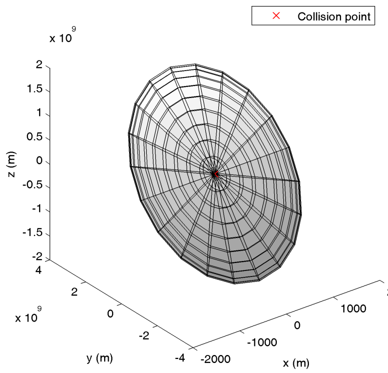

(a) Scenario 1

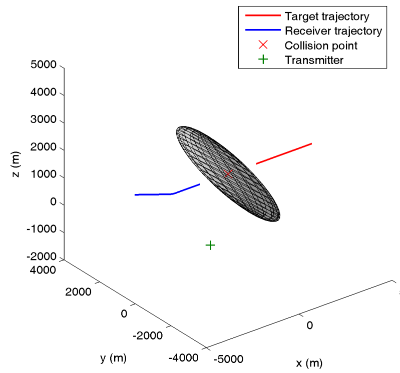

(b) Scenario 2

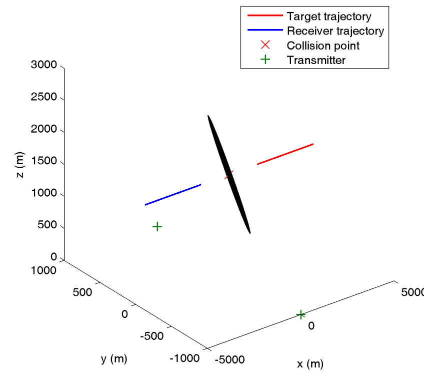

(c) Scenario 3

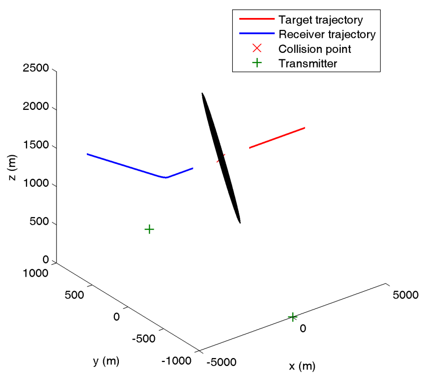

(d) Scenario 4

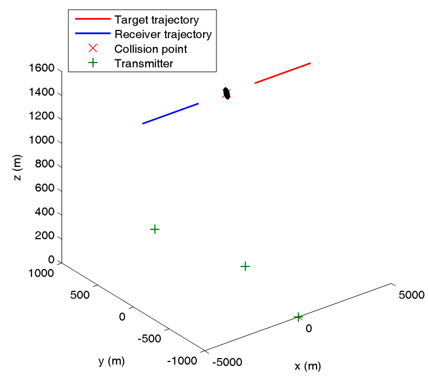

(e) Scenario 5

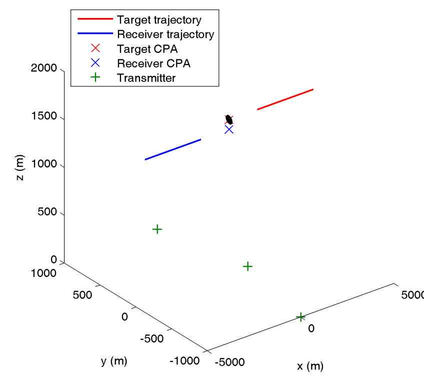

(f) Scenario 6

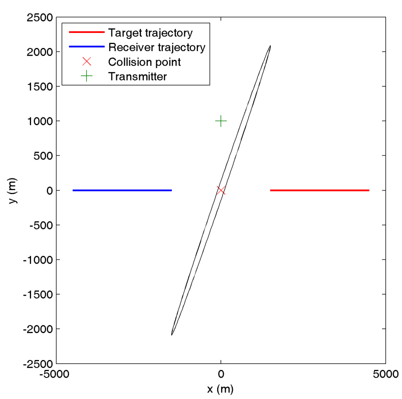

(g) Scenario 7

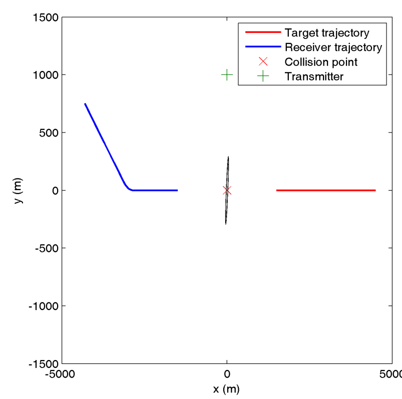

(h) Scenario 8

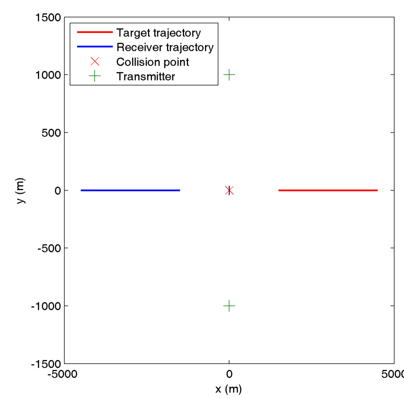

(i) Scenario 9

Fig. 2. 99.9999% uncertainty region around the collision point or the target CPA. The region is an ellipsoid in Scenarios 1 to 6 and is an ellipse in Scenarios 7 to 9. The parameter is mathematically unobservable in Scenario 1. The paramter is badly observable in Scenarios 2, 3, 4, 7 and 8. The parameter observability is good in Scenarios 5, 6 and 9.

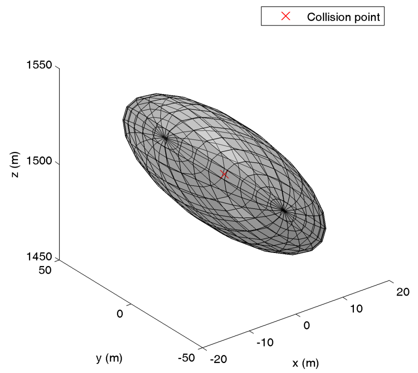

(a) Scenario 5

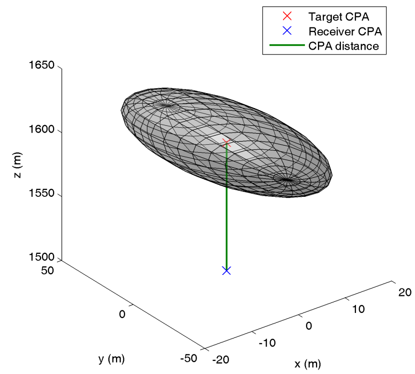

(b) Scenario 6

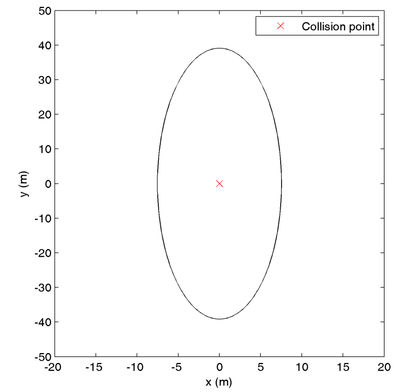

(c) Scenario 9

Fig. 3. Magnified version of 99.9999% uncertainty region around the collision point or the target CPA in Scenarios 5, 6 and 9.

where

$$\mathbf{z} = [\mathbf{z}(1)', \mathbf{z}(2)', \ldots, \mathbf{z}(N)']' \tag{30}$$

$$\mathbf{h}(\hat{\mathbf{x}}^j) = \left[\mathbf{h}(\hat{\mathbf{x}}^j, 1), \mathbf{h}(\hat{\mathbf{x}}^j, 2), \ldots, \mathbf{h}(\hat{\mathbf{x}}^j, N)\right]' \tag{31}$$

$$R = \begin{bmatrix} R(1) & \mathbf{0} & \cdots & \mathbf{0} \\ \mathbf{0} & R(2) & \cdots & \mathbf{0} \\ \vdots & \vdots & \ddots & \vdots \\ \mathbf{0} & \mathbf{0} & \cdots & R(N) \end{bmatrix} \tag{32}$$

and

$$H^j = \begin{bmatrix} [\nabla_{\mathbf{x}} \mathbf{h}(\mathbf{x}, 1)']'\big|_{\mathbf{x}=\hat{\mathbf{x}}^j} \\ [\nabla_{\mathbf{x}} \mathbf{h}(\mathbf{x}, 2)']'\big|_{\mathbf{x}=\hat{\mathbf{x}}^j} \\ \vdots \\ [\nabla_{\mathbf{x}} \mathbf{h}(\mathbf{x}, N)']'\big|_{\mathbf{x}=\hat{\mathbf{x}}^j} \end{bmatrix} \tag{33}$$

An initial estimate can be obtained by solving (3) with the noise set to zero based on the measurements for two transmitters at two different time instants.

The ML estimate of the target parameter $\mathbf{x}_{2\mathrm{D}}$ in (26) in a 2-D scenario can be found using the ILS technique in the same manner.

B. Collision Warning via Hypothesis Testing Based on a Generalized Likelihood Function

The collision event at time t (t to be determined) is defined by equating the true target position $\mathbf{x}_\mathrm{p}(t)$ to the ownship position, namely,

$$\{\text{Collision at } t\} \triangleq \{\mathbf{x}_\mathrm{p}(t) = \mathbf{s}(t)\} \tag{34}$$

Following [3], the likelihood function of collision is the pdf of the predicted target position to time t (the "observation" based on which the collision warning can be made) conditioned on (34)

$$\begin{aligned} \Lambda\left[\mathbf{x}_\mathrm{p}(t) = \mathbf{s}(t); \hat{\mathbf{x}}_\mathrm{p}(t)\right] &= p[\hat{\mathbf{x}}_\mathrm{p}(t) | \mathbf{x}_\mathrm{p}(t) = \mathbf{s}(t)] \\ &= \mathcal{N}\left[\hat{\mathbf{x}}_\mathrm{p}(t); \mathbf{s}(t), P_\mathrm{p}(t)\right] = |2\pi P_\mathrm{p}(t)|^{-1/2} \\ &\cdot \exp\left(-\frac{1}{2}(\hat{\mathbf{x}}_\mathrm{p}(t) - \mathbf{s}(t))' P_\mathrm{p}(t)^{-1} (\hat{\mathbf{x}}_\mathrm{p}(t) - \mathbf{s}(t))\right) \end{aligned} \tag{35}$$

where $\hat{\mathbf{x}}_\mathrm{p}(t)$ is given by (20). The use of the covariance $P_\mathrm{p}(t)$ in (35) is justified based on the discussion presented in Section V, which confirms that (28) is a statistically efficient estimator.

Since the time t in (35) is not known, we estimate the CPA time as

$$\hat{t}_\mathrm{CPA} = \arg\max_t \Lambda\left[\mathbf{x}_\mathrm{p}(t) = \mathbf{s}(t); \hat{\mathbf{x}}_\mathrm{p}(t)\right] \tag{36}$$

The collision warning can be formulated as a hypothesis testing problem as follows. The two hypotheses are, based on (36)

$$H_0 : \mathbf{x}_\mathrm{p}(\hat{t}_\mathrm{CPA}) = \mathbf{s}(\hat{t}_\mathrm{CPA}) \tag{37}$$

$$H_1 : \mathbf{x}_\mathrm{p}(\hat{t}_\mathrm{CPA}) \neq \mathbf{s}(\hat{t}_\mathrm{CPA}) \tag{38}$$

The (generalized[2]) likelihood function for H_0 is

$$\begin{aligned} \Lambda\left[H_0; \hat{\mathbf{x}}_\mathrm{p}(\hat{t}_\mathrm{CPA})\right] &= \mathcal{N}\left[\hat{\mathbf{x}}_\mathrm{p}(\hat{t}_\mathrm{CPA}); \mathbf{s}(\hat{t}_\mathrm{CPA}), P_\mathrm{p}(\hat{t}_\mathrm{CPA})\right] \\ &= \mathcal{N}\left[\mathbf{s}(\hat{t}_\mathrm{CPA}); \hat{\mathbf{x}}_\mathrm{p}(\hat{t}_\mathrm{CPA}), P_\mathrm{p}(\hat{t}_\mathrm{CPA})\right] \end{aligned} \tag{39}$$

Then H_0 is rejected at a level of, say, 0.0001% if $\mathbf{s}(\hat{t}_\mathrm{CPA})$ is outside the 99.9999% confidence region centered at $\hat{\mathbf{x}}_\mathrm{p}(\hat{t}_\mathrm{CPA})$, then one can say that collision is unlikely ($<$ 0.0001%). Otherwise a collision warning is issued.

[2]This is a generalized likelihood function because it relies on $\hat{t}_\mathrm{CPA}$, which is an estimate.

TABLE II
THE NUMBER OF WARNINGS IN 100 RUNS USING THE 3-D COLLISION WARNING ALGORITHM

	CPA angle			
Separation in altitude (m)	180°	165°	150°	135°
0	100	100	100	100
50	30	28	38	49
100	0	0	0	0
150	0	0	0	0
200	0	0	0	0
250	0	0	0	0
300	0	0	0	0

TABLE III
THE NUMBER OF WARNINGS IN 100 RUNS USING THE 2-D COLLISION WARNING ALGORITHM

	CPA angle			
Separation in altitude (m)	180°	165°	150°	135°
0	100	100	100	100
50	100	100	99	99
100	100	100	84	14
150	100	98	7	0
200	100	77	0	0
250	100	36	0	0
300	100	14	0	0

V. SIMULATION RESULTS

A. *Efficiency of ML Estimator of the Target Parameter*

The sample averages of the NEES for the 6-D target parameter in Scenario 5 from 100 Monte Carlo runs based on the CRLB evaluated at the truth and at the estimate are calculated. The values are 5.6244 and 5.6146, which can be considered practically identical. Both values fall inside the two-sided 95% probability region [5.34, 6.70], which confirms the validity of the CRLB as the actual covariance of the 3-D estimator. The sample averages of the NEES for the 4-D target parameter in Scenario 9 from 100 Monte Carlo runs based on the CRLB evaluated at the truth and at the estimate are also calculated. The values are 4.1169 and 4.1205, which can also be considered practically identical. Both values fall inside the two-sided 95% probability region [3.46 4.57], which confirms the validity of the CRLB as the actual covariance of the 2-D estimator. Therefore, the efficiency of the ML estimator is verified in both scenarios.

B. *Collision Warning with Estimated CPA Time*

The root mean square (RMS) error for the CPA time from 100 Monte Carlo runs in Scenarios 5, 6 and 9 is 0.023 s, 0.31 s and 0.012 s, respectively. And the corresponding maximum deviation from the true CPA time in each scenario is 0.061 s, 0.35 s and 0.032 s. The maximum deviation in position at a speed of 50 m/s is less than 20 m, which is smaller than the dimension of an airplane. Therefore, the estimation error in the CPA time is acceptable in practice.

The collision warning is "on" for all 100 runs in Scenario 5 and 9, that is, at the estimated CPA time the ownship position is inside the confidence region of the true target position around its estimate as illustrated in Figure 4(a) and 4(c). The collision warning is "off" for all 100 runs in Scenario 6, that is, at the estimated CPA time the ownship position is outside the confidence region of the true target position around its estimate as illustrated in Figure 4(b).

The term "CPA angle" is defined as the angle formed by the target velocity vector and the ownship velocity vector at the CPA time when they are projected on a plane at the same altitude. Therefore, the CPA angle is 180° in Scenario 5, 6 and 9.

The performance of the 3-D collision warning algorithm is further evaluated by varying the target and ownship altitude separation[3] from 0 to 300 m in steps of 50 m and the CPA angle from 180° to 135° in steps of -15° one parameter at a time in Scenario 5. From Table II, the performance of 3-D collision warning algorithm is not influenced by the CPA angle. It has no missed detection of a collision and has no false alarm when the intruder and ownship altitude separation is beyond 100 m when there is no collision.

The performance of the 2-D collision warning algorithm is evaluated in the same manner and the results are shown in Table III. It has no missed detection when there is indeed a collision, which is the same as the 3-D algorithm. The CPA angle is more influential in the 2-D case. Recall that in the 2-D scenarios it is assumed that the intruder is at the same altitude as the ownship, which is not true when the altitude separation is not zero. When the CPA angle is close to 180°, the collision is very likely to occur based on the same altitude assumption, the false alarm rate is therefore very high. When the CPA angle is reduced beyond 150°, the 2-D collision warning algorithm has no false alarms when the intruder and ownship altitude separation is beyond 200 m.

The warning algorithm is useful in both 3-D and 2-D scenarios. It is very accurate but more expensive using 3 transmitters. One could use two transmitters for more savings. Although the false alarm rate is very high when the CPA angle is close to 180°, the avoidance maneuver action (changing the course of the ownship by a small angle) caused by the false alarm can be readily realized because of the small size of the confidence region as shown in Figure 4(c).

VI. CONCLUSIONS

The ability to sense and avoid non-cooperative targets is essential for UAS to perform routine tasks when they are not alone in the airspace. We investigated several configurations with bistatic range and Doppler measurements for collision warning. It turned out that a multistatic configuration is needed to provide good observability of the target localization parameter, which is useful for collision avoidance. The minimum number of the transmitters required is three in a 3-D scenario and two in a 2-D scenario. We also implemented an ML estimator in both types of scenarios using the ILS technique and showed that the estimator is statistically efficient through Monte Carlo simulations. Based on the ML estimator, the

[3] 1000 ft (≈ 300 m) is a global standard for vertical separation

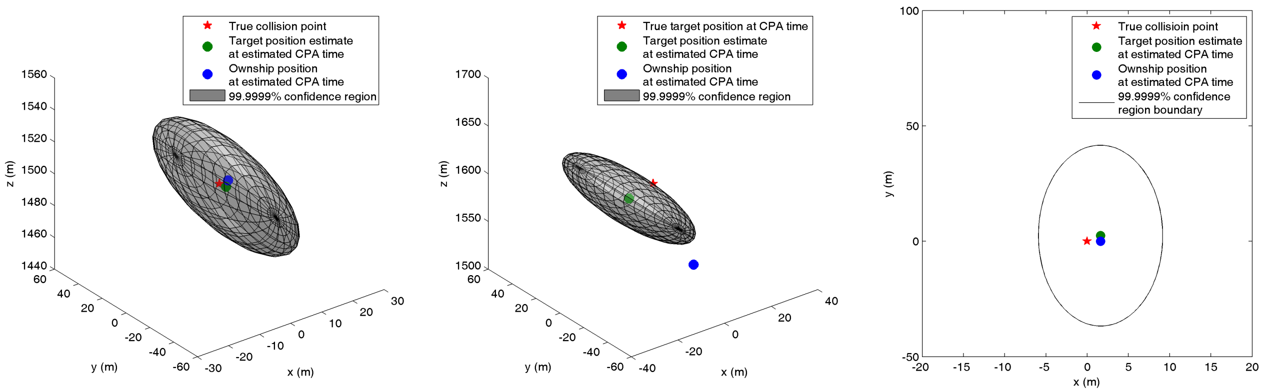

(a) Scenario 5 (b) Scenario 6 (c) Scenario 9

Fig. 4. Collision warning decisions in a single run in Scenarios 5, 6 and 9. Collison warning is "on" in Scenarios 5 and 9 and is "off" in Scenario 6.

collision warning was formulated as a hypothesis testing problem using a generalized likelihood function. The warning algorithm has no missed detection of a collision in both the 3-D and 2-D scenarios. The warning algorithm has much lower false alarm rates using the 3-D estimator than the 2-D counterpart at the expense of one more transmitter.

ACKNOWLEDGMENT

Stimulating discussions with Melissa Meyer and Robert Coury are gratefully acknowledged. This work is supported by ARO W991F-10-1-0369

REFERENCES

[1] B. Albaker and N. Rahim, "A survey of collision avoidance approaches for unmanned aerial vehicles," in *Technical Postgraduates (TECHPOS), 2009 International Conference for*, Dec 2009, pp. 1–7.

[2] Y. Bar-Shalom, P. K. Willett, and X. Tian, *Tracking and Data Fusion: A Handbook of Algorithms*. YBS Publishing, 2011.

[3] Y. Bar-Shalom, X. R. Li, and T. Kirubarajan, *Estimation with Applications to Tracking and Navigation: Theory, Algorithms and Software*. Wiley, 2001.

[4] S. Blackman and R. Popoli, *Design and Analysis of Modern Tracking Systems*. Artech House, 1999.

[5] C. Carbone, U. Ciniglio, F. Corraro, and S. Luongo, "A novel 3D geometric algorithm for aircraft autonomous collision avoidance," in *Decision and Control, Proc. 45th IEEE Conference on*, Dec 2006, pp. 1580–1585.

[6] W. Dou, P. Willett, and Y. Bar-Shalom, "Fusion of range-only measurements from multistatic configurations for air collision warning," in *Aerospace Conference, 2015 IEEE*, Big Sky, MT, March 2015.

[7] Y. Kwag and C. Chung, "UAV based collision avoidance radar sensor," in *Geoscience and Remote Sensing Symposium, IGARSS 2007. IEEE International*, July 2007, pp. 639–642.

[8] D. Sislak, M. Rehak, M. Pechoucek, D. Pavlicek, and M. Uller, "Negotiation-based approach to unmanned aerial vehicles," in *Distributed Intelligent Systems: Collective Intelligence and Its Applications, DIS 2006. IEEE Workshop on*, June 2006, pp. 279–284.

[9] C. Tomlin, J. Lygeros, and S. Sastry, "A game theoretic approach to controller design for hybrid systems," *Proceedings of the IEEE*, vol. 88, no. 7, pp. 949–970, July 2000.

[10] P. R. Williams, "Aircraft collision avoidance using statistical decision theory," *Proc. SPIE*, vol. 1694, pp. 29–34, July 1992.